scientific reports

Check for updates

OPEN

Optimization of growth and induction conditions for the production of recombinant whole cell cyclohexanone monooxygenase in *Escherichia coli*

Patrik Cabadaj[1,4], Viera Illeová[1], Hana Dobiašová[1,2], Marek Bučko[3] & Milan Polakovič[1]✉

Optimizing biocatalyst production conditions is essential for enhancing productivities and yields in biotransformation applications. This study focused on investigating the impact of the volumetric oxygen mass transfer coefficient (k_La) on the specific growth rate of recombinant *E. coli* cells and optimizing induction conditions for whole-cell cyclohexanone monooxygenase (CHMO) production. The results demonstrated that elevated k_La improved microbial growth rates, with optimal conditions achieved at k_La = 31 h^{-1}, where aerobic growth is no longer limited by dissolved oxygen. Additionally, the induction of CHMO during the exponential growth phase led to the highest specific biocatalyst activity, when used as resting cells. Further optimization of induction parameters, including the isopropyl-β-D-thiogalactopyranoside (IPTG) concentration and induction duration, significantly increased CHMO activity. The specific activity reached 54.4 U/g, representing an improvement of over 130%. Specifically, optimized conditions included a 5-hour cultivation period at k_La = 31 h^{-1}, resulting in a biocatalyst concentration of approximately 1 g/L, followed by a 20-minute induction with 0.16 mmol/L of IPTG. Bioreactor strategies for a biocatalytic Baeyer-Villiger oxidation process were evaluated, revealing that repeated batch experiments with cell washing between cycles maintained CHMO activity at 53 U/g over multiple cycles, making this the most favorable method for sustained CHMO activity and technology application. This study underscores the importance of induction optimization in maximizing biocatalyst activity for potential pilot-scale applications. These findings provide valuable insights into the optimization of biocatalytic processes, paving the way for enhanced efficiency and productivity in Baeyer-Villiger monooxygenase (BVMO)-driven processes.

Keywords Baeyer-Villiger oxidation, Cyclohexanone monooxygenase, Whole-cell biocatalyst, *E. coli* resting cells, Cultivation optimization, Induction optimization

Within the realm of biocatalysis and green chemistry, the exploitation of microbial enzymes has emerged as a potent method for the sustainable synthesis of valuable compounds. Baeyer-Villiger monooxygenases (BVMOs) have garnered substantial attention owing to their ability to facilitate the conversion of ketones into esters and lactones, utilizing air as a source of oxygen[1–3]. Realizing the full potential of BVMOs necessitates the development of efficient production platforms encompassing biocatalyst preparation[4–6], bioreactor design[6–9], and operational conditions[7–9].

Our recent study[10] utilized a genetically modified, robust *Escherichia coli* BL21(DE3)(pMM04) host for expressing cyclohexanone monooxygenase (CHMO), originally derived from *Acinetobacter sp.* NCIMB 9871[11,12]. Achieving high specific activity of whole-cell CHMOs requires meticulous attention to both reaction conditions and biocatalyst preparation procedures. Enhancing the oxygen transfer rate (OTR) positively impacts whole-

[1]Department of Chemical and Biochemical Engineering, Institute of Chemical and Environmental Engineering, Faculty of Chemical and Food Technology, Slovak University of Technology, Radlinského 9, 812 37 Bratislava, Slovakia. [2]Axxence Slovakia s.r.o, Mickiewiczova 9, 811 07 Bratislava, Slovakia. [3]Department of Glycobiotechnology, Institute of Chemistry, Slovak Academy of Sciences, Dúbravská cesta 9, 84538 Bratislava, Slovakia. [4]Present address: Sensible Biotechnologies s.r.o., Dúbravská cesta 9, 845 38 Bratislava, Slovakia. ✉email: milan.polakovic@stuba.sk

cell CHMO activity. Conversely, inadequate OTR results in limited production rates, with oxygen preferentially channeled into metabolic pathways, thereby impeding the full catalytic potential of recombinant CHMO[13–15].

Enhancing the performance of biotransformation production processes also involves optimizing the preparation procedure for whole-cell biocatalysts. Enzyme engineering methods are commonly used as the main tool for improving the activity and stability of biocatalysts, including CHMOs[16–24]. However, from the process point of view, designing optimized cultivation and induction conditions for whole-cell biocatalysts offers further possibilities to enhance the yield and catalytic activity of CHMO. The intricacies of CHMO production and the optimization of growth and induction processes were explored by drawing insights from a diverse range of induction reagents and methodologies reported in the literature[13,25–28]. The yield of active recombinant enzymes is markedly affected by the type and concentration of the induction reagent, such as isopropyl-β-D-thiogalactopyranoside (IPTG)[29–31] or more specific L-arabinose[4,9,32] considering the growth state and conditions of the production strain.

IPTG is a robust induction agent, and its concentration spans three ranges: low-level induction (0.1 mmol/L to 0.5 mmol/L) for tight gene expression control recommended for temperature inducible promoters[33], moderate induction (0.5 mmol/L to 0.8 mmol/L) balancing protein expression and cell viability, and high-level induction (over 0.8 mmol/L of IPTG) for applications demanding high protein yield. However, high-level induction often leads to heightened metabolic stress and the formation of inclusion bodies containing undesired enzymes[34–38].

Moreover, both temperature and pH, as process parameters, affect the expression of desired recombinant proteins. For effective induction, good solubility and proper folding of proteins, using the T7 promoter inducible with allolactose analogues such IPTG, a lower temperature than the optimal 37 °C for *E. coli* growth is recommended. Therefore, higher functional expression and protein stability are achievable at 25–30 °C. However, the transcriptional and translational rates are slower at these temperatures, which might result in lower overall yields of proteins[39,40].

Furthermore, a neutral pH is most favored for *E. coli* cultivation and protein expression, resulting in the most effective induction using various promoters, including T7. A pH lower than neutral or higher than 8 induces stressful conditions for the bacterial cells, which reduce the promoter activity. Conversely, a slightly alkaline pH (7.2–8) still provides good induction efficiency[39–41]. Thus, in this study, pH and temperature were adopted and not further optimized for the whole-cell CHMO production.

The primary aim of this study was to optimize the production of whole-cell CHMO, with a focus on maximizing its specific activity. This optimization process entailed exploring the impact of the volumetric oxygen transfer coefficient $k_L a$ on the growth rate, determining the optimal timing for induction initiation, identifying the specific concentration of the induction agent, and optimizing the induction duration. Subsequent to the optimization phase, the performance of the whole-cell CHMO biocatalyst was evaluated using three bioreactor strategies to assess the stability and catalytic potential of the biocatalyst. These strategies included repeated addition of substrate, continuous feeding of substrate, and repeated usage of rewashed resting cells, which are metabolically active but neither growing nor dividing.

Materials and methods

Materials

The production strain used in this study was *E. coli* BL21(DE3)(pMM04), which harbors the plasmid encoding cyclohexanone monooxygenase (CHMO) sourced from *Acinetobacter* sp. NCIMB 9871[11]. Analytical standards with the highest available purity for bicyclic lactones, (1 S,5R)-2-oxabicyclo[3.3.0]oct-6-en-3-one and (1R,5 S)-3-oxabicyclo[3.3.0]oct-6-en-2-one, and a bicyclic ketone, cis-bicyclo[3.2.0]hept-2-en-6-one, were procured from Sigma-Aldrich (Saint-Louis, MO, USA). The bacterial peptone, bacterial tryptone, and yeast extract used in the Luria-Bertani broth (LB) and terrific broth (TB) media were obtained from Oxoid (Basingstoke, UK). Glycerol and salts (K_2HPO_4, KH_2PO_4 and NaCl) were procured from Centralchem (Bratislava, Slovakia). Ampicillin (AMP) and isopropyl-β-D-thiogalactopyranoside (IPTG) were purchased from Sigma-Aldrich. A 50 mg/mL stock solution of AMP and 50 mmol/L stock of IPTG were stored in a refrigerator at -20 °C.

For cell disruption, both BugBuster Protein Extraction Reagent and urea used were procured from Sigma-Aldrich. The total protein concentration was determined using the Roti®Qunat universal kit from Carl Roth GmbH + Co. KG (Karlsruhe, Germany). Tris base, sodium dodecyl sulfate, glycerol, 2-mercaptoethanol and bromophenol blue, which are the components of Laemmli reagents for protein samples treatment, were purchased from Sigma-Aldrich. Polypeptides were separated by electrophoresis using a 4–15% Mini-PROTEAN® TGX™ precast protein gel in Tris-glycine running buffer. A BLUeye prestained protein ladder from Sigma-Aldrich was used as a protein molecular weight marker. For protein staining, ROTI®Blue staining solution from Carl Roth GmbH + Co. KG was used.

Biocatalyst production optimization at the shake-flask scale

The whole-cell biocatalyst production protocol closely followed that outlined in our previous paper[10]. Bacterial cells were stored at − 80 °C in a concentrated glycerol solution. The cell suspension was spread onto an LB-agar plate (3% w/v) and incubated for 16 h at 37 °C. Two colonies from the plate were then transferred to 25 mL of liquid LB medium (bacteriological peptone 10 g/L, yeast extract 5 g/L and sodium chloride 10 g/L), and the inoculum was grown for 12 h at 37 °C with orbital mixing set at 210 rpm in the incubator Heidolph Unimax 1010 (Heidolph Scientific Products GmbH, Germany, Schwabach). Subsequently, 1% v/v of the culture was transferred to 40–400 mL of liquid TB medium (bacteriological tryptone 12 g/L, yeast extract 24 g/L, glycerol 4 g/L, potassium phosphate monobasic 2.2 g/L, potassium phosphate dibasic 9.4 g/L) in a 500 mL Erlenmeyer flask and incubated at 210 rpm and 37 °C. The buffering capacity of the phosphate buffer proved to be sufficient with pH ranging 7.2–6.6 during the cultivation. Furthermore, the maximal oxygen transfer rate OTR_{max} was calculated using the following equation[42]:

$$OTR_{max} = 3.72\, x\, 10^{-7}\ Osmol^{0.05}\ n^{\left(1.18-\frac{Osmol}{10.1}\right)}\ V_L^{-0.74}\ d_0^{0.33}\ d^{1.88}\ p_R\ y_{O2} \quad (1)$$

where *Osmol* represents osmolality [mol/kg], n shaking frequency [rpm], V_L filling volume [mL], d_0 shaking diameter [cm], d maximum shake flask diameter [mm], p_R reactor pressure [bar], and y_{O_2} oxygen mole fraction in the gaseous phase[42]. OTR_{max} divided by the oxygen saturation concentration at 37 °C (0.211 mmol/L) gave the corresponding value of k_La.

The bacteria were allowed to grow for 2–12 h. Dry cell concentration measurements were performed in triplicate with a mean error of approximately 2%. Aliquots of the cell suspension were withdrawn during growth, and cooled to 25 °C, after which IPTG was added at concentrations ranging from 0.045 mmol/L to 1.2 mmol/L to initiate CHMO induction. The induction process was maintained for 20 min to 3 h at 25 °C and 210 rpm. After the induction process was completed, the specific activity of the whole-cell biocatalyst was determined under non-growth conditions as described in the section CHMO specific activity determination.

Additionally, each growth curve was monitored until three points in the stationary phase were acquired. The specific growth rate μ was subsequently evaluated as the slope of the linear portion of the following equation:

$$ln\ (c_X)\ =\ ln\ (c_{0,X}) + \mu\ t \quad (2)$$

where c_X [g/L] represents the dry cell concentration over time, $c_{0,X}$ [g/L] the initial dry cell concentration after inoculation (0.031 ± 0.001 g/L), μ [h^{-1}] the specific growth rate, and t [h] the cultivation time. The mean error of μ was 1.5%.

Biocatalyst preparation for bioreactor experiments

The inoculum was prepared as described in Sect. 2.2 and applied at a concentration of 1% v/v to 2 L of the TB liquid medium in a 5 L Erlenmeyer flask. The culture was allowed to grow for 5 h at 37 °C with k_La adjusted to a value of 31 h^{-1} by orbital shaking at 210 rpm (Eq. (1))[42]. Induction was conducted as described above with an IPTG concentration of 0.15 mmol/L and an induction duration of 20 min. Subsequently, 4 g/L glucose was added to impede basidial expression[43,44], and the cells containing CHMO were harvested by centrifugation. The cells were then washed twice with a saline solution (9 g/L NaCl, 0.2 g/L AMP) and resuspended in the saline at a 1:1 mass ratio. This cell suspension was used immediately in biotransformation experiments.

CHMO specific activity determination

The CHMO activity test was performed in a 20 mL double-jacket pneumatically agitated in-house bioreactor with an inner diameter of 2 cm and a working volume of 10 mL. A reaction buffer of 9.8 mL (50 mmol/L phosphate buffer, 0.2 g/L AMP, 4 g/L glucose, 0.5 g/L bicyclic ketone) and 0.2 mL of resting cell suspension (biocatalyst concentration in the bioreactor adjusted to approximately 1 g of dry cell mass per L) were added to the bioreactor. The activity test was conducted in duplicate at 25 °C using the initial rate method. Biocatalyst activity was associated with the initial rate of bicyclic lactone formation evaluated from 6 to 7 concentration values obtained during the first hour of the experiment. The concentrations of reaction components in the reaction samples were determined by GC (see section Analytical methods) and expressed in µmol/L. The initial slope of the dependence of bicyclic lactone concentration on time was determined in µmol/L/min. According to the definition of enzyme activity, a slope of 1 µmol/L/min corresponds to a CHMO activity of 1 U/L. The CHMO specific activity (per gram of dry cell mass) was calculated by dividing the CHMO activity by the biocatalyst concentration. The mean error of specific activity was approximately 3%.

Bioreactor studies

Both batch and fed-batch experiments were carried out at 25 °C in a 250 mL mechanically stirred (Rushton turbine diameter of 2.8 cm) double-jacket in-house bioreactor (inner diameter of 8.5 cm) equipped with an optical pO_2 probe Hamilton Visiferm ARC DO 225 (Hamilton, Bonaduz, Switzerland) for online dissolved oxygen concentration monitoring. In batch experiments, a reaction buffer of 150 mL (50 mmol/L phosphate buffer, 0.2 g/L AMP, 4 g/L glucose) was loaded into the bioreactor, and the bicyclic ketone substrate concentration was adjusted to 1.5 g/L or 2.5 g/L. The biotransformation experiment using the resting *E. coli* cells was initiated by adding the cell stock suspension to achieve a dry cell mass concentration of 3 g/L. To ensure the absence of oxygen limitation, the value of k_La was set to 52 h^{-1} using the stirrer frequency of 600 rpm and aeration rate of 1 vvm[10].

Fed-batch experiments began in batch mode during the first hour with an initial reaction buffer volume of 100 mL, initial bicyclic ketone concentration of 2 g/L and the same experimental conditions as in the batch experiments. Subsequently, the volumetric flowrate of the substrate feed (6 g/L bicyclic ketone, 50 mmol/L phosphate buffer, 0.2 g/L AMP) was set to 0.15 mL/min and maintained for 12 h. To ensure sufficient glucose levels, 4 g/L glucose was added every 2 h using a concentrated stock solution (500 g/L). Furthermore, a fresh cell stock suspension was added every hour to compensate for the decrease of cell concentration by its dilution by the substrate feed.

Analytical methods

Both chiral bicyclic lactone products and bicyclic ketone substrate concentrations were analyzed using an Agilent 7890 A GC (Agilent Technologies, Santa Clara, USA) instrument equipped with an HP-5 column (Agilent Technologies, USA). The bioreactor cell-containing samples were extracted with 800 µL of ethyl acetate (CG-FID purity) for 5 min. After sedimentation, the organic phase was transferred to a test tube containing the drying agent Na_2SO_4. Subsequently, the dehydrated samples were filtered through an HPTFE (hydrophobic polytetrafluoride ethane) filter, and 100 µL of the filtrate was taken to a vial through a glass insert. Forty µL of an

internal standard solution (0.172 g/L of methyl benzoate solution in ethyl acetate) was added to the filtrate and the mixture was vortexed.

One microliter of the mixture was injected into a GC. The initial temperature of each analysis was set at 40 °C, which was subsequently increased with a gradient of 35 °C/min for 2 min. This temperature was held for 3 min. A 25 °C/min gradient was subsequently applied to reach 160 °C with a hold time of two minutes. Finally, the column was cooled to 40 °C in 5 min and held for 3 min before a new sample was injected. The mean errors of bicyclic ketone and bicyclic lactone concentrations were approximately 2%.

The glucose concentration was determined using an enzymatic assay GLU-500 (Erba Lachema, Brno, Czechia). A total of 210 µL of the enzymatic assay agent was added to the wells of a 96-well plate, which were then tempered at 37 °C for 10 min. Simultaneously, a 100 µL bioreactor sample was centrifuged in an Eppendorf tube for 2 min to separate the cells. Subsequently, 10 µL of the sample supernatant was added to the agent in each well. The 96-well plate with multiple samples was inserted into a BioTek ELx808 plate reader (BioTech, Bratislava, Slovakia) where the reaction mixture was developed for 30 min at 37 °C, and the absorbance was read at 490 nm. The glucose concentration was determined from a linear calibration dependence. All analyses were performed in duplicate. The mean error of glucose concentration was 2%.

Protein concentration determination and SDS-PAGE

Ten milliliters of culture suspension at the end of cultivation was harvested by centrifugation. The resulting cell pellet was resuspended in 200 µL of BugBuster Protein Extraction Reagent and incubated for 20 min at 600 rpm at ambient temperature in a 1.5 mL test tube. Subsequently, the suspension was centrifuged at 15 000 rpm for 20 min at 4 °C, and the supernatant was collected as the soluble fraction. The insoluble part of the pellet was resuspended in 200 µL of 6 M urea and incubated for 20 min at 600 rpm and 60 °C. Then, the suspension was centrifuged at 15 000 rpm for 20 min at 4 °C, and the supernatant was collected as the insoluble fraction. The protein concentrations in the soluble and insoluble fractions were determined with the mean error of 2% using a BCA Roti®Qunat universal kit. A fraction sample (1.2 mg/mL; 20 µL) was mixed with 20 µL of 2x Laemmli reagent and heated to 90 °C for 8 min. Afterward, the solution was cooled for 2 min in the freezer and centrifuged for 1 min at 10 000 rpm and at ambient temperature. Ten microliters of the solution and 5 µL of a marker were loaded onto a 4–15% Mini-PROTEAN® TGX™ gel (200 V, 60 min, Tris-glycine buffer). The gel was stained for 1 h in ROTI®Blue staining solution and subsequently destained in deionized water for 1 h.

Results and discussion

Optimization of biocatalyst cultivation

Optimizing conditions for microorganism production, especially for biocatalytic applications, is pivotal for achieving higher conversion rates and biocatalyst yields. The initial phase of our optimization study focused on investigating the impact of oxygen mass transfer on cell growth. In aerobic cultivations, dissolved oxygen serves as the secondary substrate for growth. Increasing the oxygen transfer rate enhances the growth rate, thereby reducing the cultivation duration[45–47]. This optimization strategy aims to accelerate microbial growth and facilitate efficient substrate utilization, leading to higher conversion rates. Ultimately, optimizing the oxygen transfer rate is crucial for scaling up biocatalytic processes for industrial applications, as it enhances the productivity of the process and minimizes resource consumption and production costs[45–47].

Figure 1A demonstrates that a higher k_La during aerobic cultivation can enhance the growth rate of the production strain, resulting in a maximum specific growth rate of 0.66 h^{-1} (Fig. 1B), when glycerol is used as the carbon and energy source at a concentration of 4 g/L. For the three highest k_La values, the stationary phase was reached after 6 h. Therefore, oxygen transfer is considered the growth rate-limiting step for k_La values lower than 31 h^{-1}. Figure 1B, however, shows that the cells in the stationary phase had a lower CHMO specific activity a_m. Microorganisms in the stationary phase of growth suffer from exhaustion of essential nutrients, leading to physiological changes, and resulting in a decreased expression of the desired enzyme. Although the specific activity was approximately 10% higher at k_La = 24 h^{-1}, the cell concentration at this condition was about 30% lower (Fig. 1A). Therefore, the trade-off between the total amount of active enzyme and cell-specific activity favored k_La = 31 h^{-1}. Furthermore, k_La = 31 h^{-1} was chosen for a close investigation of the change of CHMO specific activity during the 12-hour cultivation (Fig. 2).

Figure 2 illustrates the effect of the growth phase on the CHMO specific activity. The highest activity, approximately 24 U/g, was observed during the early exponential phase of growth. However, as the culture progressed to late exponential phase and subsequently to early stationary phase, the a_m decreased. After 12 h of cultivation, the activity reached its lowest value, representing only 23% of the maximum activity. The induction of recombinant enzymes is most effective during the exponential phase due to the highest metabolic activity and optimal physiological conditions of the production strain. The depletion of essential nutrients for cell growth triggers a metabolic shift in bacteria, negatively affecting recombinant protein expression[29,48–50].

Based on the findings presented in Fig. 2, a cultivation time of 5 h and k_La = 31 h^{-1} were chosen. At this time, the maximum specific activity was still maintained, and the cell concentration reached a relatively high value of 0.96 g/L.

Optimization of CHMO induction process

To maximize the catalytic potential of whole-cell CHMO, optimizing induction conditions such as the concentration of the induction agent IPTG and induction duration is crucial. For this optimization study, cultivation was performed for 5 h at a k_La set to 31 h^{-1} as proposed in the previous section, with IPTG added at the end of cultivation. The IPTG concentration varied from 0.045 mmol/L to 1.2 mmol/L, and the induction duration ranged from 20 to 120 min. Given that the whole-cell biocatalyst concentration was 1.0 g/L, the specific IPTG dosage per dry cell mass was numerically identical to the IPTG concentration per liter of cell suspension.

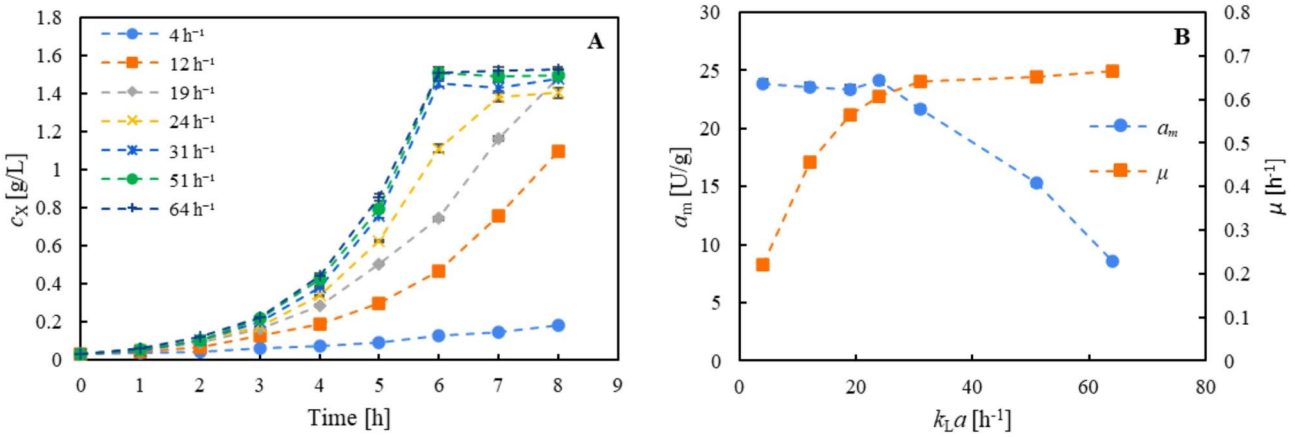

Fig. 1. Growth curves of *E. coli* BL21(DE3)(pMM04) for the range of k_La 4–64 h^{-1} at a glycerol concentration of 4 g/L for the first 8 h of cultivation (**A**) and dependence of CHMO specific activity a_m and specific growth rate μ versus k_La (**B**). The induction was initialized after 6 h of cultivation by adding 0.25 mmol IPTG per 1 g of dry cell mass for 3 h.

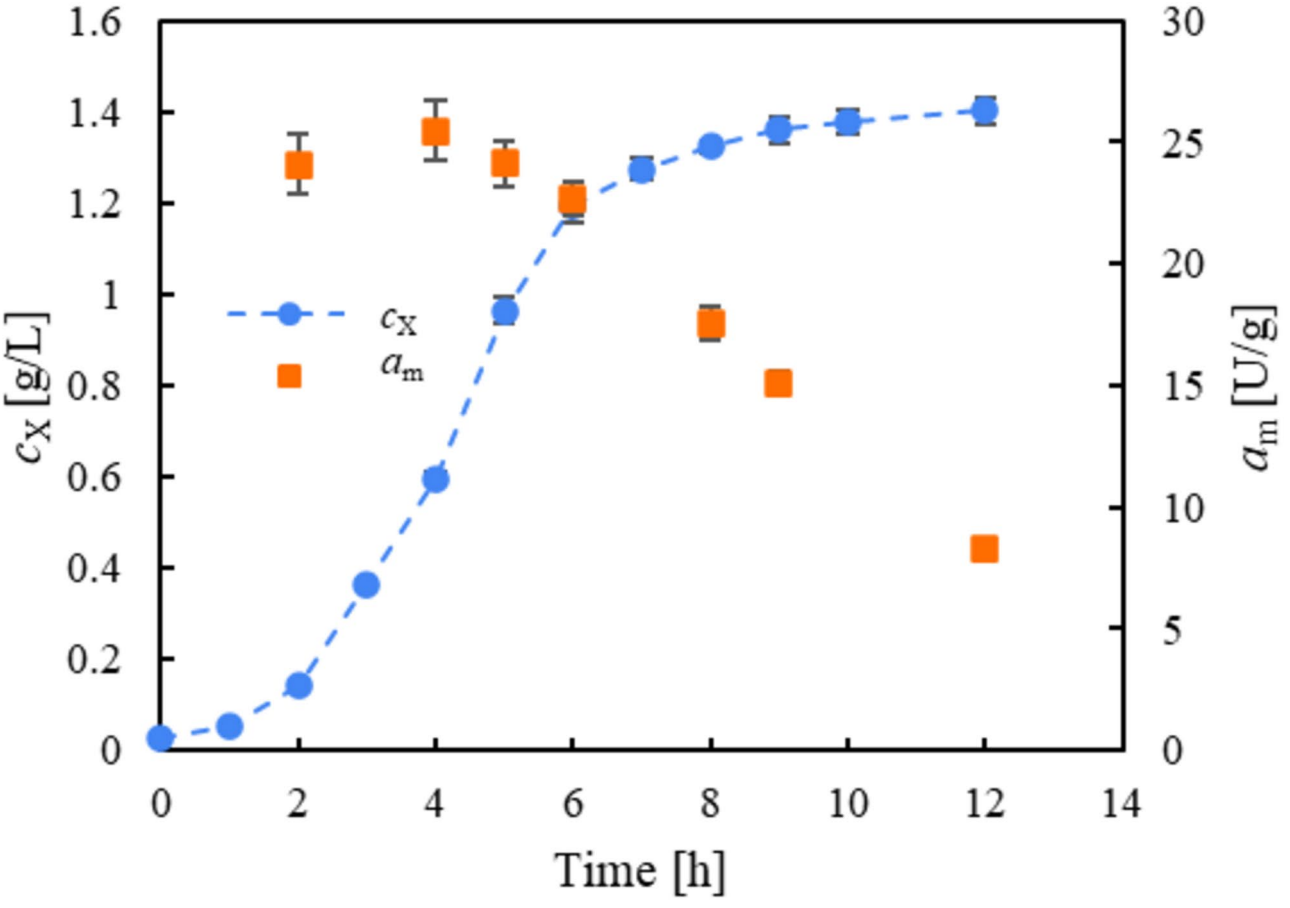

Fig. 2. CHMO specific activity for cells induced at various times of cultivation conducted at k_La = 31 h^{-1}. The induction process was initialized by adding 0.25 mmol of IPTG per 1 g of dry cell mass and lasted 3 h.

Figure 3 depicts the correlation between the CHMO specific activity a_m and the optimized parameters. The results demonstrated that the CHMO specific activity is dependent on both the induction duration and IPTG concentration. A distinct maximum a_m was observed at an IPTG concentration of approximately 0.15 mmol/L. This value implies that the T7 promoter belongs to the low-level induction category with respect to IPTG. Moderate-level induction conditions can cause undesirable phenomena with respect to CHMO expression[39,51].

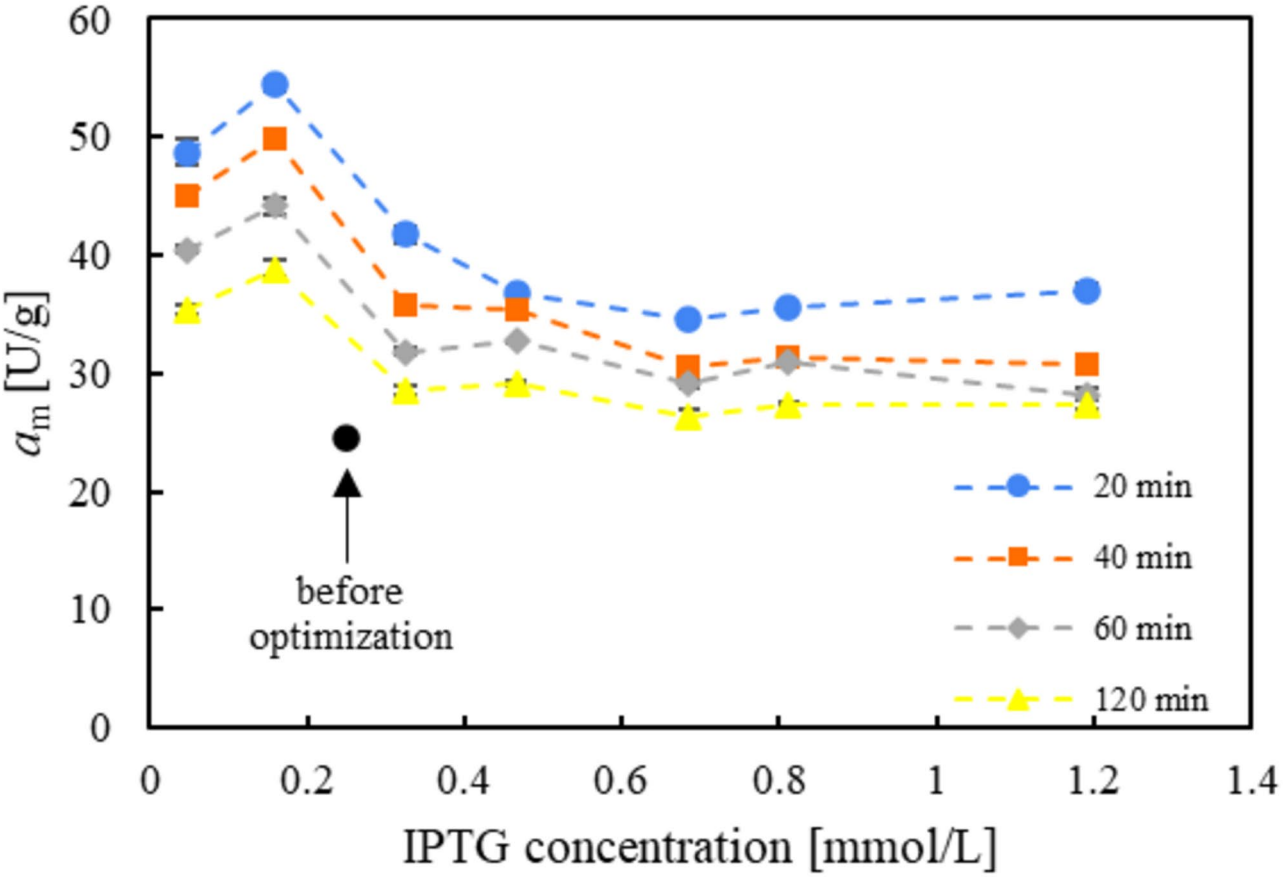

Fig. 3. CHMO specific activity vs. IPTG concentration with induction duration as a curve parameter. Induction was initialized after 5 h of cultivation at $k_L a = 31\ h^{-1}$ with a biocatalyst concentration of 1.0 g/L.

The highest value of a_m presented in Fig. 3 is 54.4 U/g, representing an increase of more than 130% compared to the value of 23.7 U/g before induction optimization. It can also be concluded that the optimized biocatalyst is approximately twice as active as previously reported for the BV oxidation of the bicyclic ketone[4]. This improvement in the CHMO induction process is very promising for the potential scale-up of BV oxidation.

Figure 3 illustrates that this significant enhancement in whole-cell CHMO activity was primarily achieved by shortening the induction duration from 3 h to 20 min and, to a lesser extent, by reducing the IPTG dosage from 0.25 mmol/g to 0.15 mmol/L. The optimal induction duration is significantly shorter that of other published BVMO induction procedures, for which the induction duration was 6–24 h[52–55]. In this context, it can be inferred that the expression of CHMO occurs rapidly, with induction periods exceeding 20 min yielding no additional active CHMO synthesis. On the contrary, CHMO specific activity decreased. A prolonged induction process probably led to the formation of inactive CHMOs.

Additional quantitative data on CHMO formation can be inferred from the total protein concentrations presented in Table 1. They were determined in the soluble and insoluble fractions of cell homogenates for three different induction durations: 0 min (immediately after IPTG addition), 20 min, and 180 min. These fractions were also examined via SDS-PAGE to detect potential alterations in the molecular structure of CHMO and other cellular proteins (Fig. 4).

The results presented in Table 1 show that the sum of the total protein concentration in the soluble (samples D-F) and insoluble fractions (samples J–L) increased from the initial value of about 9.5 g/L to 11.4 g/L for the 20-minute induction. The total protein concentration remained then unchanged for the 180-minute induction although a change in the protein distribution between the soluble and insoluble fractions was observed. However, the lanes corresponding to samples D-F and J–L in Fig. 4 do not exhibit any significant effect on the distribution of protein sizes in the soluble and insoluble fractions, respectively.

The mean position of CHMO bands was identified at 62 kDa, which aligns with the reported value of 61.6 kDa reported for *Acinetobacter* sp. CHMO expressed in *E. coli*[56,57]. Upon comparing the intensity of CHMO bands across different induction durations, a correlation with the total protein concentration is evident. The presence of CHMO before induction may result from leaky expression, a common characteristic of the T7 promoter system due to basal activity of the T7 RNA polymerase even in the absence of IPTG[58]. Specifically, CHMO levels appear to increase in the soluble fraction with increasing induction duration, but reach a peak at the 20-minute induction for the insoluble fraction. The decrease in CHMO concentration in the insoluble fraction at longer induction durations explains the reduction in whole-cell specific activity discussed above.

Soluble fraction				Insoluble fraction			
Sample	t_{ind} [min]	c_{PMSF} [mmol/L]	c_{prot} [g/L]	Sample	t_{ind} [min]	c_{PMSF} [mmol/L]	c_{prot} [g/L]
A	0	0.5	7.50 ± 0.13	G	0	0.5	1.84 ± 0.02
B	20	0.5	8.05 ± 0.34	H	20	0.5	2.06 ± 0.04
C	180	0.5	9.84 ± 0.38	I	180	0.5	2.89 ± 0.09
D	0	x	7.83 ± 0.11	J	0	x	1.75 ± 0.03
E	20	x	8.40 ± 0.28	K	20	x	3.04 ± 0.13
F	180	x	9.41 ± 0.40	L	180	x	1.88 ± 0.06

Table 1. Total protein concentration c_{prot} in the soluble (samples A-F) and insoluble (samples G-L) fractions of cell proteins for various induction durations, t_{ind}, and concentrations of added PMSF, c_{PMSF}. The values after the plus/minus sign are the standard deviations. More details are given in the legend of Fig. 4.

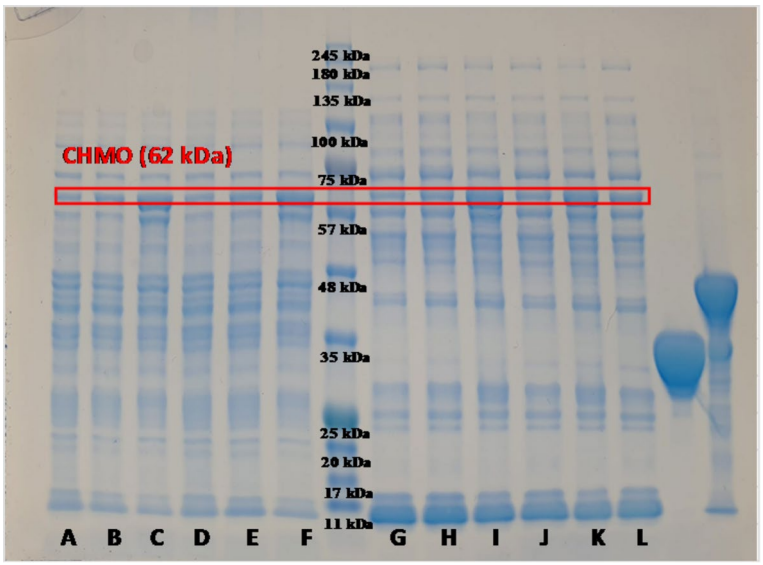

Fig. 4. Effect of protease activity suppression on CHMO (62 kDa) and other biocatalyst proteins by PMSF addition at the beginning of induction, with induction duration as the parameter, examined via SDS-PAGE. The middle lane represents the molecular weight markers of the protein standard solution (0–245 kDa). Lanes to the left of the middle correspond to soluble fractions of the biocatalyst proteins whereas the lanes to the right correspond to insoluble fractions. The characteristics of the samples were as follows: (A) and (G) 0 min induction and PMSF addition, (B) and (H) 20 min induction and PMSF addition, (C) and (I) 180 min induction and PMSF addition, (D) and (J) 0 min induction without PMSF addition, (E) and (K) 20 min induction without PMSF addition, and (F) and (L) 180 min induction without PMSF addition. This gel is cropped. The original gel, including two samples unrelated to this study, is shown in the Supplementary Information.

The CHMO molecule is rich in cysteine (6 residues) and serine (12 residues) residues[59]. Adding an inhibitor of serine/cysteine proteases, such as phenylmethylsulphonyl fluoride (PMSF), to the medium during induction should suppress the possible decomposition of synthesized CHMO[60–62]. This approach was employed to protect CHMO from potential proteolytic degradation, thereby ensuring its stability during the induction period. To test this possibility, the impact of adding 0.5 mmol/L PMSF at the beginning of the induction period was examined for the same three induction durations as in the previous experiments. The results obtained are presented in Fig. 4; Table 1, along with those without PMSF addition. Evidently, the PMSF addition had a negligible effect on the CHMO band intensity, protein size distribution and total concentration in the soluble fraction (samples A-C).

Additionally, at an induction time of 0 min, the band corresponding to CHMO was noticeable, suggesting that the plasmid undergoes leaky expression of the desired protein even in the absence of IPTG. This indicates that the promoter exhibits basal activity, potentially due to factors such as incomplete repression by the *lac*I repressor, a high plasmid copy number, or unintended transcriptional readthrough. Despite the lack of induction, the specific activity of the biocatalyst of 6.24 U/g was observed, confirming the presence of functionally active CHMO.

A different picture emerged for the insoluble fraction (Fig. 4; Table 1). Here, unlike in the experiments without PMSF addition, no peak in CHMO band intensity or protein concentration was observed at the induction

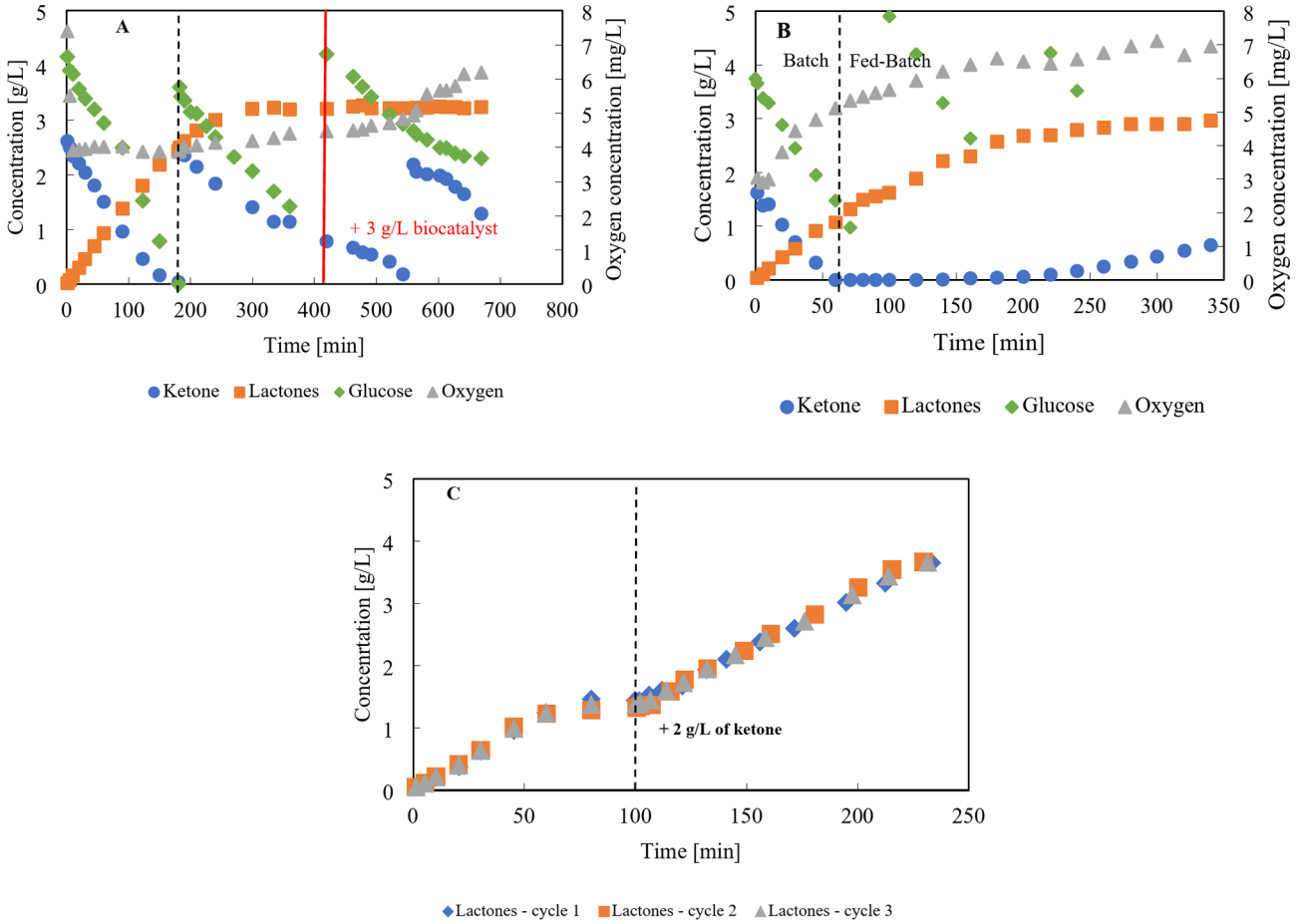

Fig. 5. Progress curves for three bioreactor strategies for resting whole-cell CHMO application with the initial glucose and dry cell mass concentration of 4 g/L and 3 g/L, respectively, and k_La of 52 h^{-1}: (**A**) Repeated addition of 2.5 g/L bicyclic ketone. The vertical lines indicate the timing of ketone and glucose additions. Additionally, the red line marks the time point at which 3 g/L of biocatalyst was added and kLa was increased to 104 h^{-1}; (**B**) Continuous feeding of 6 g/L bicyclic ketone stock at a volumetric flow rate of 0.15 mL/min. The dashed vertical line marks the end of the initial batch operation mode and the beginning of the fed-batch mode. If glucose symbols are absent at certain times, it indicates that glucose concentrations exceeded 5 g/L; and (**C**) Repeated use of the biocatalyst in three batches with an initial bicyclic ketone concentration of 1.5 g/L. The dashed vertical line marks the point at which fresh ketone substrate was added at a concentration of 2 g/L.

duration of 20 min (samples G-I). Conversely, both variables increased with induction duration. However, the protein concentration at 180 min with PMSF addition was still lower than that at 180 min without PMSF. This finding indicates that while PMSF inhibits the decomposition of CHMO over time, it also slows its expression. Therefore, the addition of PMSF was not considered for the optimized biocatalyst production procedure, which was set as follows: 5-hour cultivation at k_La = 31 h^{-1}; 0.15 mmol/L IPTG addition, and an induction duration of 20 min.

Bioreactor strategies

The performance of the optimized biocatalyst for BV oxidation was examined in three bioreactor strategies. Only batch and fed-batch modes were investigated in this study, as the continuous mode faces severe problems with CHMO biocatalyst stability as was shown in our previous work[10]. Figure 5 illustrates the comparison of these three bioreactor strategies. As shown in Fig. 5A, a straightforward strategy of substrate addition (approximately 2.5 g/L) effectively mitigated ketone toxicity. However, despite successfully reaching a lactone concentration of 3.3 g/L, the production rate eventually decreased to zero.

Notably, while metabolic pathways exhibited sustained activity, as indicated by continued glucose consumption, no further lactones were produced. An essential observation emerged when scrutinizing the rate of glucose consumption: when metabolism and BV oxidation were adequately sustained, the ratio between the molar glucose consumption rate and the molar lactone production rate reached a stoichiometric ratio of 1:1.

The lactone progress curve illustrates the decrease in CHMO specific activity during the course of biotransformation. The initial value of a_m was evaluated to be 52.2 U/g. After the first addition of 2.5 g/L substrate, the a_m was halved, and upon the formation of 3.3 g/L lactones, the specific activity reached zero.

Hence, at 420 min into the reaction, 3 g/L of fresh biocatalyst was added in an attempt to restore CHMO activity. To ensure sufficient oxygen transport at the twofold biocatalyst concentration, the value of k_La was also doubled.

However, CHMO activity was not recovered, suggesting very strong inhibition at a bicyclic lactone concentration of 3.3 g/L. Nevertheless, the concentration of bicyclic ketone consistently decreased with no lactone production observed. Therefore, the progress curves of bicyclic ketone and lactones indicate nonbiocatalytic consumption of bicyclic ketone. We hypothesize that this phenomenon may be attributed to two mechanisms: either the accumulation of ketone in both the cell membrane and the cytoplasm, or biosorption[63–65]. An elevated concentration of ketone or lactone in the cytoplasm could inhibit the production of bicyclic lactone, as a result of either substrate or product inhibition. However, the glucose and oxygen progress curves demonstrated the maintenance of cell metabolism.

Figure 5B illustrates the second strategy, which is based on continuous substrate feeding. Initially, the bioreactor was operated in batch mode for 60 min, after which the ketone substrate stock (6 g/L) was continuously fed at a volumetric flow rate of 0.15 mL/min. To maintain a constant biocatalyst concentration and ensure sufficient glucose levels during the fed-batch phase, an appropriate cell suspension was added to the bioreactor every hour, and 4 g/L glucose was added every 200 min.

The initial value of a_m during the batch phase was essentially the same as that in the previous strategy (52.7 U/g). Following the transition to the fed-batch phase, the ketone concentration remained at zero for more than 140 min. Thus, this strategy of continuous feeding avoided potential substrate inhibition problems inherent to the previous strategy of repeated substrate additions. BV oxidation was well-maintained, with a mean value of a_m = 28.8 U/g in this phase. Moreover, the evaluated ratio of the molar glucose consumption rate to the lactone production rate remained at 1:1. The deceleration of BV oxidation is also demonstrated by the increase in the dissolved oxygen concentration.

However, the final outcome of the continuous feeding strategy mirrored that of the previous approach. After 280 min, the lactone concentration reached 3.3 g/L, and BV oxidation ceased. The biocatalyst remained metabolically active, as evidenced by the continued consumption of glucose and oxygen. Unlike in the previous strategy, ketone accumulation was not apparent in this case, as the ketone concentration increased due to its continuous supply with the feed. Therefore, any feeding strategy can enhance the productivity of this BV oxidation reaction only if it is combined with product removal techniques.

The third strategy focused on the repeated use of the CHMO biocatalyst in simple batch experiments. Figure 5C shows the concentration of the chiral bicyclic lactone mixture over time for three repeated cycles. The biotransformation began with an initial substrate concentration of 1.5 g/L to achieve 100% conversion in approximately 75 min with the total product formation rate of 1.2 g/L/h. After 100 min, an additional 2 g/L ketone was added, resulting in the lactone concentration reaching the threshold of 3.6 g/L without substrate inhibition. The separated and washed resting cells were reused for another biotransformation cycle. As shown in Fig. 5C, the concentration profiles of the lactones remained consistent, with no loss in biocatalyst activity, which was maintained at 53 U/g. Thus, this strategy stands out as the most promising for further optimization and scale up.

Conclusions

In this study, whole-cell CHMO biocatalyst production was optimized, and three bioreactor strategies for applying this biocatalyst in the BV oxidation of a bicyclic ketone were examined. An investigation of the effect of oxygen mass transfer on the specific growth rate of *E. coli* BL21(DE3)(pMM04) cells showed that bacterial growth was not limited by oxygen transfer at k_La-values of 31 h^{-1} or greater. Furthermore, the biocatalyst specific activity started to decline significantly during the late exponential phase of growth. Therefore, a 5-hour cultivation followed by a 3-hour induction was found to be optimal, representing a good compromise between the maximum cell yield and maximum specific biocatalyst activity.

At this stage of the investigation, the biocatalyst specific activity was 24 U/g. By optimizing the induction process, after the cultivation conditions were set to 5 h at k_La = 31 h^{-1}, with the IPTG concentration and induction duration as parameters, a biocatalyst with a specific activity of 54.4 U/g was obtained. Specifically, a lower IPTG concentration of 0.15 mmol/L and a shorter induction duration of 20 min led to a biocatalyst with a specific activity 130% greater than that of its nonoptimized variant. SDS-PAGE and total protein measurements of the biocatalyst developed for different induction durations confirmed the hypothesis that CHMO could be degraded if the induction duration was extended beyond 20 min. This degradation could have been impeded by the addition of PMSF, but this would slow CHMO expression.

This optimized biocatalyst was applied to the BV oxidation of a bicyclic ketone using three bioreactor strategies. Two fed-batch modes, employing either repeated additions of substrate stock or continuous feeding, were not very effective due to limitations in sustaining the CHMO biocatalyst activity over prolonged periods. Strong inhibition of BV oxidation by the formed chiral bicyclic lactones occurred at a concentration of 3.3 g/L. In contrast, utilizing repeated batch experiments with cell washing between cycles, proved to be the most promising method. This strategy maintained CHMO activity at 53 U/g over multiple cycles without any loss, highlighting its potential for large-scale applications that could economically benefit from prolonged biocatalyst lifetime. These findings contribute to the advancement of whole-cell biocatalysis and offer guidance for the development of efficient and sustainable biocatalytic BV oxidation processes.

Data availability

Data will be made available on request from the corresponding author.

Received: 25 September 2024; Accepted: 21 April 2025

Published online: 25 April 2025

References

1. Stewart, J. D. Cyclohexanone monooxygenase: A useful reagent for asymmetric Baeyer-Villiger reactions. *Curr. Org. Chem.* **2**, 195–216 (1998).
2. Leisch, H., Morley, K. & Lau, P. C. K. Baeyer-villiger monooxygenases: more than just green chemistry. *Chem. Rev.* **111**, 4165–4222 (2011).
3. Balke, K., Kadow, M., Mallin, H., Saß, S. & Bornscheuer, U. T. Discovery, application and protein engineering of Baeyer-Villiger monooxygenases for organic synthesis. *Org. Biomol. Chem.* **10**, 6249–6265 (2012).
4. Doig, S. D., Simpson, H., Alphand, V., Furstoss, R. & Woodley, J. M. Characterization of a Recombinant *Escherichia coli* TOP10 [pQR239] whole-cell biocatalyst for stereoselective Baeyer-Villiger oxidations. *Enzyme Microb. Technol.* **32**, 347–355 (2003).
5. Doig, S. D., O'Sullivan, L. M., Patel, S., Ward, J. M. & Woodley, J. M. Large scale production of cyclohexanone monooxygenase from *Escherichia coli* TOP10 pQR239. *Enzyme Microb. Technol.* **28**, 265–274 (2001).
6. Doig, S. D. et al. Reactor operation and scale-up of whole cell Baeyer-Villiger catalyzed lactone synthesis. *Biotechnol. Prog.* **18**, 1039–1046 (2002).
7. Hilker, I. et al. Preparative scale Baeyer-Villiger biooxidation at high concentration using Recombinant *Escherichia coli* and in situ substrate feeding and product removal process. *Nat. Protoc.* **3**, 546–554 (2008).
8. Hilker, I., Alphand, V., Wohlgemuth, R. & Furstoss, R. Microbial transformations, 56. Preparative scale asymmetric baeyer-villiger oxidation using a highly productive 'two-in-one' resin-based in situ SFPR concept. *Adv. Synth. Catal.* **346**, 203–214 (2004).
9. Baldwin, C. V. F., Wohlgemuth, R. & Woodley, J. M. The first 200-L scale asymmetric Baeyer-Villiger oxidation using a whole-cell biocatalyst. *Org. Process. Res. Dev.* **12**, 660–665 (2008).
10. Cabadaj, P. et al. Investigation of process stability of a whole-cell biocatalyst with Baeyer–Villiger monooxygenase activity in continuous bioreactors. *Environ. Technol. Innov.* **30**, 103083 (2023).
11. Mihovilovic, M. Enzyme mediated Baeyer-Villiger oxidations. *Curr. Org. Chem.* **10**, 1265–1287 (2006).
12. Bučko, M. et al. Continuous testing system for Baeyer-Villiger biooxidation using Recombinant *Escherichia coli* expressing cyclohexanone monooxygenase encapsulated in polyelectrolyte complex capsules. *Enzyme Microb. Technol.* **49**, 284–288 (2011).
13. Baldwin, C. V. F. & Woodley, J. M. On oxygen limitation in a whole cell biocatalytic Baeyer-Villiger oxidation process. *Biotechnol. Bioeng.* **95**, 362–369 (2006).
14. Schrewe, M., Julsing, M. K., Bühler, B. & Schmid, A. Whole-cell biocatalysis for selective and productive C–O functional group introduction and modification. *Chem. Soc. Rev.* **42**, 6346–6377 (2013).
15. Doig, S. D., Pickering, S. C. R., Lye, G. J. & Woodley, J. M. The use of microscale processing technologies for quantification of biocatalytic Baeyer-Villiger oxidation kinetics. *Biotechnol. Bioeng.* **80**, 42–49 (2002).
16. Bocola, M. et al. Converting phenylacetone monooxygenase into Phenylcyclohexanone monooxygenase by rational design: towards practical Baeyer-Villiger monooxygenases. *Adv. Synth. Catal.* **347**, 979–986 (2005).
17. Brondani, P. B., De Gonzalo, G., Fraaije, M. W. & Andrade, L. H. Selective oxidations of organoboron compounds catalyzed by Baeyer-Villiger monooxygenases. *Adv. Synth. Catal.* **353**, 2169–2173 (2011).
18. De Gonzalo, G., Mihovilovic, M. D. & Fraaije, M. W. Recent developments in the application of Baeyer-Villiger monooxygenases as biocatalysts. *ChemBioChem* **11**, 2208–2231 (2010).
19. De Gonzalo, G., Torres Pazmiño, D. E., Ottolina, G., Fraaije, M. W. & Carrea, G. Oxidations catalyzed by phenylacetone monooxygenase from Thermobifida fusca. *Tetrahedron: Asymmetry*. **16**, 3077–3083 (2005).
20. Franceschini, S. et al. Exploring the structural basis of substrate preferences in Baeyer-Villiger monooxygenases: insight from steroid monooxygenase. *J. Biol. Chem.* **287**, 22626–22634 (2012).
21. van Beek, H. L., de Gonzalo, G. & Fraaije, M. W. Blending Baeyer-Villiger monooxygenases: using a robust BVMO as a scaffold for creating chimeric enzymes with novel catalytic properties. *Chem. Commun.* **48**, 3288–3290 (2012).
22. Mascotti, M. L., Lapadula, W. J. & Ayub, M. J. The origin and evolution of Baeyer - Villiger monooxygenases (BVMOs): an ancestral family of flavin monooxygenases. *PLoS One*. **10**, 10–27 (2015).
23. Mascotti, M. L., Ayub, M. J., Dudek, H., Sanz, M. K. & Fraaije, M. W. Cloning, overexpression and biocatalytic exploration of a novel Baeyer-Villiger monooxygenase from Aspergillus fumigatus Af293. *AMB Express*. **3**, 1–10 (2013).
24. Bisagni, S. et al. Enhancing the activity of a Dietzia Sp. D5 Baeyer-Villiger monooxygenase towards cyclohexanone by saturation mutagenesis. *ChemistrySelect* **2**, 7169–7177 (2017).
25. Shitu, J. O., Woodley, J. M., Wnek, R., Chartrain, M. & Hewitt, C. J. Induction studies with *Escherichia coli* expressing Recombinant interleukin-13 using multi-parameter flow cytometry. *Biotechnol. Lett.* **31**, 577–584 (2009).
26. Lee, W. H., Park, J. B., Park, K., Kim, M. D. & Seo, J. H. Enhanced production of ε-caprolactone by overexpression of NADPH-regenerating glucose 6-phosphate dehydrogenase in Recombinant *Escherichia coli* harboring cyclohexanone monooxygenase gene. *Appl. Microbiol. Biotechnol.* **76** (2007).
27. Mallin, H., Wulf, H. & Bornscheuer, U. T. A self-sufficient Baeyer-Villiger biocatalysis system for the synthesis of ε-caprolactone from cyclohexanol. *Enzyme Microb. Technol.* **53**, 283–287 (2013).
28. Kaufmann, H., Mazur, X., Marone, R., Bailey, J. E. & Fussenegger, M. Comparative analysis of two controlled proliferation strategies regarding product quality, influence on tetracycline-regulated gene expression, and productivity. *Biotechnol. Bioeng.* **72**, 592–602 (2001).
29. Kilikian, B. V., Suárez, I. D., Liria, C. W. & Gombert, A. K. Process strategies to improve heterologous protein production in *Escherichia coli* under lactose or IPTG induction. *Process. Biochem.* **35**, 1019–1025 (2000).
30. Dvorak, P. et al. Exacerbation of substrate toxicity by IPTG in *Escherichia coli* BL21(DE3) carrying a synthetic metabolic pathway. *Microb. Cell. Fact.* **14**, 235–249 (2015).
31. Gomes, L., Monteiro, G. & Mergulhão, F. The impact of IPTG induction on plasmid stability and heterologous protein expression by *Escherichia coli* biofilms. *Int. J. Mol. Sci.* **21**, 576 (2020).
32. Hilker, I. et al. On the influence of oxygen and cell concentration in an SFPR whole cell biocatalytic Baeyer-Villiger oxidation process. *Biotechnol. Bioeng.* **93**, 1138–1144 (2006).
33. Briand, L. et al. A self-inducible heterologous protein expression system in *Escherichia coli*. *Sci. Rep.* **6**, 33037 (2016).
34. Marbach, A. & Bettenbrock, K. Lac Operon induction in *Escherichia coli*: systematic comparison of IPTG and TMG induction and influence of the transacetylase LacA. *J. Biotechnol.* **157**, 82–88 (2012).
35. Miroux, B. & Walker, J. E. Production of proteins in *Escherichia coli*_mutant hosts that allow synthesis of some membrane proteins and globular proteins at high levels. *J. Mol. Biol.* **260**, 289–298 (1996).
36. Dong, H., Nilsson, L. & Kurland, C. G. Gratuitous overexpression of genes in *Escherichia coli* leads to growth Inhibition and ribosome destruction. *J. Bacteriol.* **177**, 1497–1504 (1995).
37. Hoffmann, F. & Rinas, U. Stress induced by Recombinant protein production in *Escherichia coli*. *Adv. Biochem. Eng. Biotechnol.* **89**, 73–92 (2004).
38. Hayat, S. M. G., Farahani, N., Golichenari, B. & Sahebkar, A. Recombinant protein expression in *Escherichia coli* (*E.coli*): what we need to know. *Curr. Pharm. Des.* **24**, 718–725 (2018).
39. Mühlmann, M., Forsten, E., Noack, S. & Büchs, J. Optimizing Recombinant protein expression via automated induction profiling in microtiter plates at different temperatures. *Microb. Cell. Fact.* **16**, 220 (2017).

40. Aucoin, M. G. et al. Identifying conditions for inducible protein production in *E. coli*: combining a fed-batch and multiple induction approach. *Microb. Cell. Fact.* **5**, 27 (2006).
41. Valdez-Cruz, N. A., Caspeta, L., Pérez, N. O. & Ramírez, O. T. Trujillo-Roldán, M. A. Production of Recombinant proteins in *E. coli* by the heat inducible expression system based on the phage lambda pL and/or pR promoters. *Microb. Cell. Fact.* **9**, 18 (2010).
42. Meier, K. et al. Correlation for the maximum oxygen transfer capacity in shake flasks for a wide range of operating conditions and for different culture media. *Biochem. Eng. J.* **109**, 228–235 (2016).
43. Epstein, W., Rothman-Denes, L. B. & Hesse, J. Adenosine 3',5'-cyclic monophosphate as mediator of catabolite repression in Escherichia coli. *Proc. Natl. Acad. Sci. USA*. **72**, 2300–2304 (1975).
44. Saier, M. H. Jr. & Ramseier, T. M. The catabolite repressor/activator (Cra) protein of enteric bacteria. *J. Bacteriol.* **178**, 3411–3417 (1996).
45. Valgepea, K., Adamberg, K. & Vilu, R. Decrease of energy spilling in *Escherichia coli* continuous cultures with rising specific growth rate and carbon wasting. *BMC Syst. Biol.* **5**, 106 (2011).
46. Kensy, F., Engelbrecht, C. & Büchs, J. Scale-up from microtiter plate to laboratory fermenter: evaluation by online monitoring techniques of growth and protein expression in *Escherichia coli* and *Hansenula polymorpha* fermentations. *Microb. Cell. Fact.* **8**, 68 (2009).
47. Shahzadi, I. et al. Scale-up fermentation of *Escherichia coli* for the production of Recombinant endoglucanase from *Clostridium thermocellum*. *Sci. Rep.* **11**, 7145 (2021).
48. Walton, A. Z. & Stewart, J. D. An efficient enzymatic Baeyer-Villiger oxidation by engineered *Escherichia coli* cells under non-growing conditions. *Biotechnol. Prog.* **18**, 262–268 (2002).
49. Walton, A. Z. & Stewart, J. D. Understanding and improving NADPH-dependent reactions by nongrowing *Escherichia coli* cells. *Biotechnol. Prog.* **20**, 403–411 (2004).
50. Kaur, J., Kumar, A. & Kaur, J. Strategies for optimization of heterologous protein expression in *E. coli*: roadblocks and reinforcements. *Int. J. Biol. Macromol.* **106**, 803–822 (2018).
51. Rudroff, F., Alphand, V., Furstoss, R. & Mihovilovic, M. D. Optimizing fermentation conditions of Recombinant *Escherichia coli* expressing Cyclopentanone monooxygenase. *Org. Process. Res. Dev.* **10**, 599–604 (2006).
52. Song, J. W. et al. Multistep enzymatic synthesis of long-chain α,ω-dicarboxylic and ω-hydroxycarboxylic acids from renewable fatty acids and plant oils. *Angew Chem. – Int. Ed.* **52**, 2534–2537 (2013).
53. Kirschner, A., Altenbuchner, J. & Bornscheuer, U. T. Cloning, expression, and characterization of a Baeyer-Villiger monooxygenase from Pseudomonas fluorescens DSM 50106 in *E. coli*. *Appl. Microbiol. Biotechnol.* **73**, 1065–1072 (2007).
54. Rehdorf, J., Kirschner, A. & Bornscheuer, U. T. Cloning, expression and characterization of a Baeyer-Villiger monooxygenase from Pseudomonas putida KT2440. *Biotechnol. Lett.* **29**, 1393–1398 (2007).
55. Riebel, A. et al. Expanding the set of rhodococcal Baeyer-Villiger monooxygenases by high-throughput cloning, expression and substrate screening. *Appl. Microbiol. Biotechnol.* **95**, 1479–1489 (2012).
56. Cheesman, M. J. et al. Purification and characterization of hexahistidine-tagged cyclohexanone monooxygenase expressed in *Saccharomyces cerevisiae* and *Escherichia coli*. *Protein Expr Purif.* **21**, 81–86 (2001).
57. Cheesman, M. J., Kneller, M. B. & Rettie, A. E. Critical role of histidine residues in cyclohexanone monooxygenase expression, cofactor binding and catalysis. *Chem. Biol. Interact.* **146**, 157–164 (2003).
58. Du, F. et al. Regulating the T7 RNA polymerase expression in *E. coli* BL21 (DE3) to provide more host options for Recombinant protein production. *Microb. Cell. Fact.* **20**, 189 (2021).
59. UniProt Consortium. Cyclohexanone 1,2-monooxygenase (Acinetobacter sp.). UniProt database. (2024). Retrieved from https://www.uniprot.org/uniprotkb/P12015/
60. García-Carreño, F. L. Protease Inhibition in theory and practice. *Biotechnol. Ed.* **3**, 145–150 (1992).
61. Li, S. H. J. et al. *Escherichia coli* translation strategies differ across carbon, nitrogen and phosphorus limitation conditions. *Nat. Microbiol.* **3**, 939–947 (2018).
62. Tunlid, A. & Jansson, S. Proteases and their involvement in the infection and immobilization of nematodes by the nematophagous fungus *Arthrobotrys oligospora*. *Appl. Environ. Microbiol.* **57**, 2868–2872 (1991).
63. Dotto, G. L. & Pinto, L. A. A. Analysis of mass transfer kinetics in the biosorption of synthetic dyes onto *Spirulina platensis* nanoparticles. *Biochem. Eng. J.* **68**, 85–90 (2012).
64. Costa, F., Quintelas, C. & Tavares, T. Kinetics of biodegradation of diethylketone by *Arthrobacter viscosus*. *Biodegradation* **23**, 81–92 (2012).
65. Suteu, D., Blaga, A. C., Diaconu, M. & Malutan, T. Biosorption of reactive dye from aqueous media using *Saccharomyces cerevisiae* biomass. Equilibrium and kinetic study. *Centr Eur. J. Chem.* **11**, 2048–2057 (2013).

Acknowledgements

The authors thank Prof. Marko D. Mihovilovič (TU Vienna, Austria) for providing the bacterial strain used in this work and dr. Peter Gemeiner (Institute of Chemistry, Slovak Academy of Sciences) for valuable advice.

Author contributions

P.C., V.I., and M.P. designed the concept of the investigation. P.C., V.I., and H.D. developed and tested the methods used, and carried out the experiments. V.I. took care of the resources for this investigation. P.C. carried out the formal analysis and data curation. P.C. and V.I. validated the results. P.C. handled the visualization of the results and wrote the original draft of the manuscript. P.C. and M.P. revised and edited the manuscript. M.B. and M.P. managed the project and are responsible for the acquisition of funding.

Declarations

Competing interests

The authors declare no competing interests.

Additional information

Supplementary Information The online version contains supplementary material available at https://doi.org/10.1038/s41598-025-99461-3.

Correspondence and requests for materials should be addressed to M.P.